Applied Energy 128 (2014) 82–92

Contents lists available at ScienceDirect

Applied Energy

journal homepage: www.elsevier.com/locate/apenergy

An improved PSO-based charging strategy of electric vehicles in electrical distribution grid

Jun Yang [a,*], Lifu He [a], Siyao Fu [b]

[a] School of Electrical Engineering, Wuhan University, Wuhan 430072, PR China
[b] Department of Electrical, Computer, and Biomedical Engineering, University of Rhode Island, RI 02881, United States

HIGHLIGHTS

- A charging model of EVs based on optimal power flow (OPF) is developed.
- EV owners' degree of satisfaction and operation cost of power grid are considered.
- An improved particle swarm optimization (PSO) algorithm is proposed.
- The performance of the optimized charging strategy is verified by simulation results.
- The global search capability and optimal result of the algorithm is validated.

ARTICLE INFO

Article history:
Received 6 February 2014
Received in revised form 24 March 2014
Accepted 13 April 2014

Keywords:
Optimal charging strategy
Electric vehicle
Improved particle swarm optimization
Optimal power flow
EV owners' degree of satisfaction

ABSTRACT

Driven by the desire to reduce environmental impacts and achieve energy independence, electric vehicles (EVs) are poised to receive mass acceptance from the general public. However, simultaneously connecting to electric distribution grid and charging with large number of EVs bring the necessity of optimizing the charging and discharging behaviors of EVs, due to the security and economy issue of the grid operation. To address this issue, we propose a novel EV charging model in this paper. The model concerns with following aspects, including optimal power flow (OPF), statistic characteristics of EVs, EV owners' degree of satisfaction (DoS), and the power grid cost. An improved particle swarm optimization (PSO) algorithm is proposed for the model optimization. To evaluate our proposed optimal EV charging strategy, a 10-bus power distribution system simulation is performed for performance investigation. Simulation results show that the proposed strategy can reduce the operational cost of the power grid considerately, while meeting the EV owner's driving requirement. Also, better performance on the global search capability and optimal result of the improved particle swarm optimization algorithm is verified.

Contents

* Corresponding author. Address: School of Electrical Engineering, Wuhan University, Luo-jia-shan, Wuchang District, Wuhan City, Hubei 430072, PR China. Tel.: +86 13995638969; fax: +86 2768772047.
E-mail address: JYang@whu.edu.cn (J. Yang).

http://dx.doi.org/10.1016/j.apenergy.2014.04.047
0306-2619/

1. Introduction

Electric vehicles (EVs) are the inevitable trend in the automotive industry's development of energy-saving and environmentally friendly cars [1–8]. EV technology presents a good option for significant reductions in gasoline consumption, smog precursors and the emission of greenhouse gases. When connected to the electric distribution grid, the power flow between EV and power grid can be bidirectional; a charging EV is a load on the grid, whereas a discharging EV is a power source [9–14]. However, if large numbers of EVs connect to the grid simultaneously, some important issues including the EV concentration at a certain location at a given time, its level of charging, SOC of battery and the charger characteristics should be considered. For example, the power quality of power grid will be affected by EV charging [15,16], such as the THD (Total Harmonic Distortion) of the total current and the voltage. According to the analysis of voltage violations, power losses and line loading, there are significant impacts on distribution networks due to EVs charging [17–19]. Without a comprehensive and effective EV charging control system, undesirable increases in peak power demand will exhaust the available capacity in the grid [20], and the electrical power network cannot be prepared to respond to these requests. All in all, power quality, lines and equipment overloading, increased grid power losses, supply demand imbalances, and instability problems are among the most serious impacts introduced by EVs [21,11,22]. Also, EVs need a long charging period to ensure a fully charged battery from the EV owner's perspective. Therefore, the coordination of the charging and discharging is necessary to optimize the operation of power grid and to meet driving demand of EV owners.

There are some existing literatures about smart charging strategies of EVs. [23] discusses an improved strategy to perform the discharge (and charge) of the batteries for its life-time point-of-view. Several EVs' coordinated charging control strategies are studied in [24–26], but only public charging stations are considered without the impacts on the power grid. A power system stochastic economic dispatch model is constructed in [27], which includes EVs and wind turbines, but the power grid constraints are not considered. Following the concept of spot prices in an electrical market, a centralized charging strategy of plug-in hybrid electric vehicles (PHEVs) is proposed based on demand side response in [28], but the vehicle-to-grid (V2G) strategy is not involved. The literature [29] evaluates the coordinated operation of EVs with conventional thermal power and wind turbines, but the transmission loss and power grid security constraints are not considered. The power system economic dispatch strategy involving the EVs charging and discharging is studied in [30–32]. However, the EV charging and discharging power constraints are ignored. A charging optimization method considering both EV charging demand and voltage constraints is proposed in [33] to minimize the power losses of distribution systems, and a linearly constrained convex quadratic programming model is constructed at each iteration by correcting nodal voltages iteratively. An optimal charging model for replacement of an EVs' battery to consider the minimum user charge cost and daily load curve fluctuation is introduced in [34,35], but V2G has not been considered yet. The study in [36] proposes data mining technology to extract electricity market prices and historical information to reduce user costs to assist the charging behavior of EVs. [37] proposes EV smart charging strategies based on the forecast of future electricity prices and dynamic programming algorithms. [38-40] present a time-coordinated optimal power flow strategy to control charging and discharging of EVs without considering the impacts of EV charging on grid security. Literature [41] formulates a globally optimal scheduling scheme, in which the charging powers are optimized to minimize the total cost of all EVs which perform charging and discharging during the day. Because the optimization problem is a convex optimization problem, it can be solved efficiently with interior point methods. Literature [42] shows that EVs can balance the electricity demand and promote the wind power integration. Literature [43] studies an optimization problem of scheduling EV charging with energy storage considering both the day-ahead and real-time markets, and a MILP model based heuristic algorithm is proposed to solve the problem in polynomial time, but EVs discharging and EV owners' benefit are not mentioned. From the perspective of an aggregator, literature [44] discusses how to manage the electricity market participation of a vehicle fleet and presents a framework for optimizing EVs charging and discharging in electricity spot prices with different driving patterns of vehicle fleet, while grid network loss and SOC of EVs are ignored. By formulating the optimization problem as a linear program, literature [45] proposes a smart charging algorithm which offers significant financial benefits to customers and aggregators for different battery replacement costs, and additional system flexibility as well as peak load reductions are also observed, but the cost of grid control equipment is not involved. In order to minimize the charging cost, literature [46] proposes a heuristic method to solve the optimized model for controlling EV charging loads in response to time-of-use (TOU) price in a regulated market, but V2G is not involved. Literature [47] proposes a novel method of planning the charging of electric drive vehicles including electricity grid constraints. Also, this method establishes an individual charging plan for each vehicle and avoids distribution grid congestion while satisfying the requirements of the individual vehicle owners.

Based on the concept of V2G, we present a new approach to optimize the charging behavior of EVs within a power grid, where both the EV owners and the power grid are considered. In Section 2, according to the stochastic characteristics of EVs, an optimal objective model based on optimal power flow is developed, which includes the EV owners' degree of satisfaction (DoS), the smoothness of the power daily load curve, the reducing loss of active power transmission and the adjustment of the power grid control equipment. In addition, the model considers the network constraints, the on-load tap changer (OLTC) transformer constraints, the transmission power constraints, the charging and discharging power constraints and the EVs' state of charge (SOC) constraints. In Section 3, an improved particle swarm optimization (IPSO) algorithm based on genetic variation is proposed. In Section 4, simulations based on a practical distribution power grid are presented to investigate the performance of the proposed charging strategy. Concluding remarks are given in Section 5.

2. The optimal EV charging–discharging model

2.1. Electric vehicle model

The charging time of EVs is affected by the owner's preference which includes their driving demand and other factors. Statistical

data of a car's usage show that private cars are sitting 95% of the day. To generate extra revenue, EV owners can transmit energy to a power grid in the vehicle's sitting time for bulk energy, spinning reserves and frequency regulation. EVs are connected to the grid in the parking time, so the characteristic curve of the number of EVs connected to the grid in one day is basically a certain profile. The time when EVs disconnect from power grid obeys a normal distribution at commuting time while following a uniform distribution in the vehicle's remaining time [17,20]. The variable $P_{leave,\beta}$ is the probability when EVs disconnect from grid at time β, thus $P_{r\beta} \approx 1 - P_{leave,\beta}$, which is the proportion of EVs connected to the grid at time β.

Generally, EVs need to travel longer distance and consume more power in commuting time (8:00–10:00 am and 3:00–6:00 pm), while EVs consume less power in rest time of a day. So EV's consumption power distribution in a day is shown in Fig. 1 [39].

After charging from the power grid to recharge the battery, the surplus energy of EVs can be returned to the grid to serve the power grid operation. To track the battery's SOC, we define a variable $E^{store}_{\alpha,\beta}$ as the remaining energy in the battery in the following equation. Assuming that EVs connected to the power grid are on the same node as an energy storage unit with bidirectional power flow:

$$E^{store}_{\alpha,\beta+1} = E^{store}_{\alpha,\beta} + P_{r\beta} \cdot N_{\alpha,EV} \cdot P^{EV}_{\alpha,\beta} \cdot \Delta t - (1 - P_{r\beta}) \cdot E^{v2r}_{\beta} \quad (1)$$

where $E^{store}_{\alpha,\beta}$ and $E^{store}_{\alpha,\beta+1}$ represent the remaining energy of EVs on node α at time β and time $\beta+1$, respectively. $N_{\alpha,EV}$ represents the number of EVs of node α, $P_{r\beta}$ represents the proportion of EVs connected to power grid at time β, E^{v2r}_{β} represents the energy possibly depleted by EVs for driving at the moment β, $P^{EV}_{\alpha,\beta}$ represents the charging or discharging power of EVs on node α from time β to time $\beta+1$, and Δt (Unit: hour) is the time interval between β and $\beta+1$.

2.2. The optimal charging strategy model

To optimize the charging and discharging behavior of a large number of EVs connected to power grid, the objective function consists of four objectives, which will be described in detail as follows.

Power grid companies prefer to reduce the power loss in transmission to lower the cost of the power grid operation; therefore, reducing power loss is an objective. So the optimization objective of power loss g_1 is denoted as

$$g_1 = \sum_{\beta=1}^{n_\beta} \sum_{\alpha=1}^{n_l} P_{Loss,\alpha\beta} \quad (2)$$

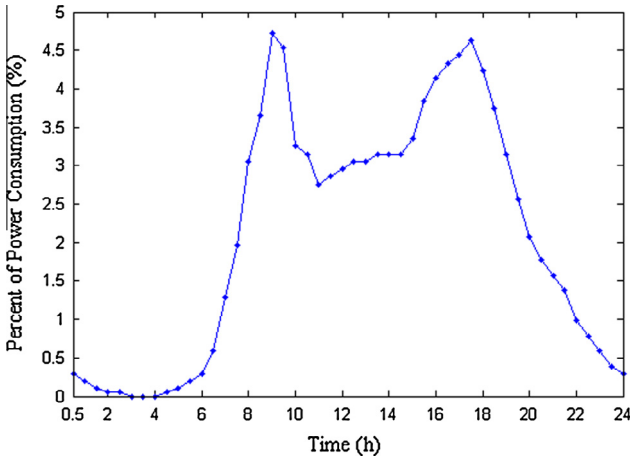

Fig. 1. The percent of EV's power consumption in a day in urban area.

where n_l is the number of branches included in the power grid, n_β is the total number of time intervals in one day, $P_{Loss,\alpha\beta}$ is the active power loss of branch α at time β.

When EVs are connected to power grid for charging and discharging, the OLTC transformers and other grid control equipment must adjust frequently to ensure the safe operation of the power grid. However, frequent operation will shorten the life of such equipment and increase the cost of the grid operation. Therefore, minimizing the changing frequency of the OLTC tap position is one of the objectives of power grid optimal operation. So the optimization objective of adjustment frequency for power grid control equipment g_2 is denotes as

$$g_2 = \sum_{\beta=1}^{n_\beta} \sum_{\alpha=1}^{n_t} \left| |t|_{\alpha\beta} - 1 \right| \quad (3)$$

where n_t is the number of transformers, $|t|_{\alpha\beta}$ is the ratio of OLTC α at time β.

From the view of the power grid, grid operation desires a smooth distribution of the daily load. After an ideal load curve based on the average daily load curve is defined, we can minimize the deviation from the actual load to the ideal load. So the optimization objective of the smoothness for the power daily load curve g_3 is denotes as

$$g_3 = \sum_{\beta=1}^{n_\beta} (P_\beta - \overline{P})^2 \quad (4)$$

where P_β is the total power grid load at time β, and $\overline{P}$ is the average load in one day without EVs.

The role of EV owners is also important in the interaction of the power grid and the EV. From the EV owners' point of view, the EV owners' DoS should be an optimization objective. When the EV leaves the power grid, the EV owner hopes that the energy in battery remains as much as possible, so the same to SOC. That is to say, SOC means EV owner's DoS. The optimization objective of EV owners' DoS g_4 can be denoted as

$$g_4 = 1 - \frac{\sum_{\alpha=1}^{n} \gamma_{\alpha 7}}{n} \quad (5)$$

where $\gamma_{\alpha 7}$ is the SOC of the EV on node α at 7:00 am, and n is the number of nodes in the power grid. Higher EV owners' DoS correlates to a lower g_4. In order to go to work in 7:00 am, the EV owner will not discharge to power grid to remain energy in battery. After 7:00 am, the EV can discharge to power grid if the owner stays at home or work place. At this time, the EV must remain enough energy to meet the owner's traveling need in the future, so γ must be greater than 0.6 (at least 60% of the energy remained in battery).

We can put all the optimization objectives together, so the optimization for charging and discharging behavior of a large number of EVs connected to power grid is considered as a multi-objective optimization problem. Because there is no mutual coupling between each optimization objective, the multi-objective optimization problem can be transformed into a single objective optimization by weighted linear combination in Eq. (6).

$$\min f = \varepsilon_1 \cdot g_1 + \varepsilon_2 \cdot g_2 + \varepsilon_3 \cdot g_3 + \varepsilon_4 \cdot g_4 \quad (6)$$

where ε_1 is the weight of g_1, ε_2 is the weight of g_2, ε_3 is the weight of g_3, ε_4 is the weight of g_4. g_1, g_2 and g_3 represent the economics of grid operation respectively, and they are equally important according to the experience of power grid operator. While g_4 represents customers DoS, it is less important than grid operation because of the practical situation in China. So we set ε_1, ε_2 and ε_3 as 0.3, and ε_4 is set as $1 - 0.3 * 3 = 0.1$.

Table 1
The parameters of constraints.

Definition	Symbol	Definition	Symbol
Injection active power at node α	$P_{G\alpha}$	Injection reactive power at node α	$Q_{G\alpha}$
Active load at node α	$P_{D\alpha}$	Reactive load at node α	$Q_{D\alpha}$
Active power transmission of node α	$P_{T\alpha}$	Reactive power transmission of node α	$Q_{T\alpha}$
Maximum ratio of OLTC α	$\|t\|_{\alpha,\max}$	Minimum ratio of OLTC α	$\|t\|_{\alpha,\min}$
Ratio of OLTC α	$\|t\|_{\alpha}$	EV's charging power at node α	P_{α}^{EV}
Maximum of EV's charging power at point α	$P_{\alpha,\max}^{EV}$	Maximum of EV's discharging power at point α	$\|P_{\alpha,\min}^{EV}\|$
Maximum voltages of node α	$V_{\alpha,\max}$	Minimum voltages of node α	$V_{\alpha,\min}$
Voltage of node α	V_{α}	Active power transmission of line l	P_l
Active power transmission limit of line l	$P_{l,\max}$	Remaining energy of EV on node α	E_{α}^{store}
EV's battery capacity at node α	$E_{\alpha,\max}^{store}$		

The following constraints in our optimization problem must be satisfied at each time interval β, and the definitions of related parameters are shown in Table 1.

$$P_{G\alpha} - P_{D\alpha} - P_{T\alpha} = 0 \tag{7}$$

$$Q_{G\alpha} - Q_{D\alpha} - Q_{T\alpha} = 0 \tag{8}$$

$$|t|_{\alpha,\min} \leqslant |t|_{\alpha} \leqslant |t|_{\alpha,\max} \tag{9}$$

$$P_{\alpha,\min}^{EV} \leqslant P_{\alpha}^{EV} \leqslant P_{\alpha,\max}^{EV} \tag{10}$$

$$V_{\alpha,\min} \leqslant V_{\alpha} \leqslant V_{\alpha,\max} \tag{11}$$

$$|P_l| \leqslant P_{l,\max} \tag{12}$$

$$E_{\alpha}^{store} \geqslant 0.1 * E_{\alpha,\max}^{store} \tag{13}$$

Eqs. (7) and (8) indicate the active and reactive power balance constraints of the nodes. Eq. (9) indicates the transformer ratio restraint. Eq. (10) represents the EV's charging and discharging power constraint, while $P_{\alpha}^{EV} > 0$ represents EV charging and $P_{\alpha}^{EV} < 0$ represents EV discharging. Eq. (11) represents the node voltage amplitude constraint, and Eq. (12) is the branch's transmission power constraint. The life of an EV's battery will be shortened due to the over-discharge of the battery, so the status of charging batteries is constrained by Eq. (13) according to [48-50].

Based on $|t|_{\alpha}$ and P_{α}^{EV}, V_{α}, P_l and E_{α}^{store} can be derived after power flow calculation of Eq. (14). The power flow of grid can be controlled by the charging and discharging power of EVs and the ratio of adjustable transformers, so $|t|_{\alpha}$ and P_{α}^{EV} are control variables, V_{α}, P_l and E_{α}^{store} are state variables.

$$\begin{cases} P_{T\alpha} = V_{\alpha}\sum_{j\in\alpha} V_j(G_{\alpha j}\cos\theta_{\alpha j} + B_{\alpha j}\sin\theta_{\alpha j}) \\ Q_{T\alpha} = V_{\alpha}\sum_{j\in\alpha} V_j(G_{\alpha j}\sin\theta_{\alpha j} - B_{\alpha j}\cos\theta_{\alpha j}) \\ |P_l| = |P_{ij}| = |V_i V_j(G_{ij}\cos\theta_{ij} + B_{ij}\sin\theta_{ij}) - V_i^2 G_{ij}| \\ P_{Loss,l} = P_{ij} + P_{ji} \\ P_{loss,km} = |V_k|^2|t|^2 G_{km} + |V_m|^2 G_{km} - 2|V_k||V_m||t|G_{km}\cos\theta_{km} \end{cases} \tag{14}$$

where V_{α} and V_j are voltages of node α and j, respectively. $G_{\alpha j}$ is the conductance between node α and node j, and $B_{\alpha j}$ is the susceptance between node α and node j. $\theta_{\alpha j}$ is the phase angle difference between node α and node j. $P_{Loss,l}$ is the active power loss of branch l. $P_{loss,km}$ is the active power loss of the branch between node k and node m with an OLTC, and $|t|$ is the ratio of OLTC.

The matrix of control variables is denoted as follows:

$$u_i = \begin{bmatrix} P_{11}^{EV} & P_{12}^{EV} & \cdots & P_{1n_\beta}^{EV} \\ \vdots & \vdots & \vdots & \vdots \\ P_{n1}^{EV} & P_{n2}^{EV} & \cdots & P_{nn_\beta}^{EV} \\ |t|_{11} & |t|_{12} & \cdots & |t|_{1n_\beta} \end{bmatrix}_i \tag{15}$$

3. Improved particle swarm optimization (IPSO) based on gene algorithm and simulated annealing

The key of the optimization model for EVs charging and discharging is how to solve the optimal power flow (OPF) model, which is a nonlinear, non-convex, large-scale, static optimization problem with both continuous and discrete control variables. The exact algorithms, such as Linear Programming, Nonlinear Programming and Interior Point Methods, can be applied to solve traditional OPF problem. These methods rely on convexity to obtain the global optimum solution and as such are forced to simplify relationships in order to ensure convexity [51]. However, the EVs' charging and discharging problem is non-convex due to the existence of the nonlinear AC power flow equality constraints. So the exact algorithms are not guaranteed to converge to the global optimum of the non-convex OPF problem [52]. Also, the presence of discrete control variables, such as transformer tap positions, further complicates the solution. The particle swarm optimization (PSO) algorithm can overcome the limitations of non-convex and discrete control variables, and it has some advantages such as simplicity, easy realization, fewer parameters and fast convergence compared with traditional optimization algorithms (and including meta-heuristics algorithms). Furthermore, its ability of global optimum can be improved. Therefore, it is a good choice to implement EV charging and discharging strategy.

A penalty function method is usually applied to inequality constraints, but the determination of such a penalty factor in our case is difficult. If the penalty factor is too large, it may lead to a lack of convergence; meanwhile, a small penalty factor will make such a penalty useless. An improper penalty function method may even cause the annihilation of the particles [53].

In this paper, a feasible reservation strategy is applied to handle the inequality constraints. It is assumed that the feasible region defined in the constraints of our charging and discharging model is F and the number of particles in the swarm is N. When particle i advances to generation k, its evolution position is denoted as $u_i^k = (u_{i1}^k, u_{i2}^k, \ldots, u_{iD}^k)$ which is the control variable matrix, and its fitness value is denoted as $f(u_i^k)$. The best location in its search history is $p_i^k = (p_{i1}^k, p_{i2}^k, \ldots, p_{iD}^k)$, and the best fitness value in its search history is $f(p_i^k)$. The best position of the group's evolution in generation k is $g^k = (g_1^k, g_2^k, \ldots, g_D^k)$.

The initial value of the position of the particles is randomly generated. To increase the probability of searching the global optimal solution by following the particle in this space, it is necessary to make all initialized particles uniformly distributed in the feasible region during the population initialization. The best position of each particle and group will be updated only when the searched solution falls into the feasible region and when it is better than the previous solution. The feasible reservation strategy only allows a feasible solution to guide the particle flight because a search of

the particle in the infeasible region is deemed invalid; therefore, the calculation efficiency of the algorithm is improved.

The development of best position of particle i based on its search history is as follows:

$$p_i^k = \begin{cases} u_i^k, (u_i^k \in F) \cap (f(u_i^k) < f(p_i^{k-1})) \\ p_i^{k-1}, (u_i^k \notin F) \cup (f(u_i^k) \geqslant f(p_i^{k-1})) \end{cases} \quad (16)$$

The equation of the group's development is as follows:

$$g^k = \min(p_1^k, p_2^k, \ldots, p_N^k) \quad (17)$$

Each particle updates its position based on its own best exploration, best swarm overall experience, and its previous velocity according to the following model:

$$v_{id}^k = w v_{id}^{k-1} + c_1 \times rand_1 \times (p_{id}^k - u_{id}^{k-1}) + c_2 \times rand_2 \times (g_d^k - u_{id}^{k-1}) \quad (18)$$

$$u_{id}^k = u_{id}^{k-1} + v_{id}^k \quad (19)$$

where $i = 1, 2, \ldots, N$, N is the population size of PSO. $d = 1, 2, \ldots, D$, D is the dimension of the search space. c_1 and c_2 are two positive constants. $rand_1$ and $rand_2$ are two randomly generated numbers in a range of [0,1], w is the inertia weight, p_{id}^k is the best position particle i based on its own experience, g_d^k is the best position based on overall swarm's experience and k is the iteration index.

In an iterative version of PSO, the variable w is the inertia factor. A large w means better a global search ability of the PSO, while a small w means better local search ability. To balance the global search ability and the local search ability [54], this paper uses a linear decreasing function in the iterative process.

$$w = w_{\max} - ((w_{\max} - w_{\min})/k_{\max}) \times k \quad (20)$$

where $w_{\max}$ is the initial value and $w_{\min}$ is the ending value, $k_{\max}$ is the maximum number of iterations, and k is the current number of iterations.

The main disadvantage of PSO algorithm is that it is difficult to get the optimal global solution. To overcome this difficulty, this paper applies a Gaussian mutation in a genetic algorithm (GA) to force some particles to mutate, and it applies the annealing mechanism of a simulated annealing algorithm to accept the adverse mutation with certain probability [55,56]. As a result, the diversity of particles is increased and the global search ability is improved.

In each evolution, a specified number of particles are randomly selected to mutate based on the probability of mutation.

$$u'_{id} = u_{id}[1 + \xi] \quad (21)$$

where u'_{id} is the new position of particle i after a mutation, and ξ is the random number obeying the standard normal distribution. An acceptance of the mutation depends on the annealing mechanism of simulated annealing algorithm after the fitness value calculation.

$$\left.\begin{matrix} f'_i = f(u'_{id}) \\ f_i = f(u_{id}) \end{matrix}\right\} \Delta f = f'_i - f_i \quad (22)$$

$$u_{id} = \begin{cases} u'_{id}, \min(1, e^{-\Delta f/T}) > \zeta \\ u_{id}, \text{other} \end{cases} \quad (23)$$

where T is the annealing temperature, and ζ is the random variable with a standard uniform distribution from 0 to 1. In Eq. (23), if $\Delta f \leqslant 0$, u_{id} is replaced by u'_{id} with probability of 1. If $\Delta f > 0$, u_{id} is replaced by u'_{id} with probability of $e^{-\Delta f/T}$ [55].

The cooling schedule is calculated as follows.

$$T_k = \lambda T_{k-1} \quad (24)$$

where T_k is the annealing temperature of the kth iteration, λ is the coefficient of cooling temperature.

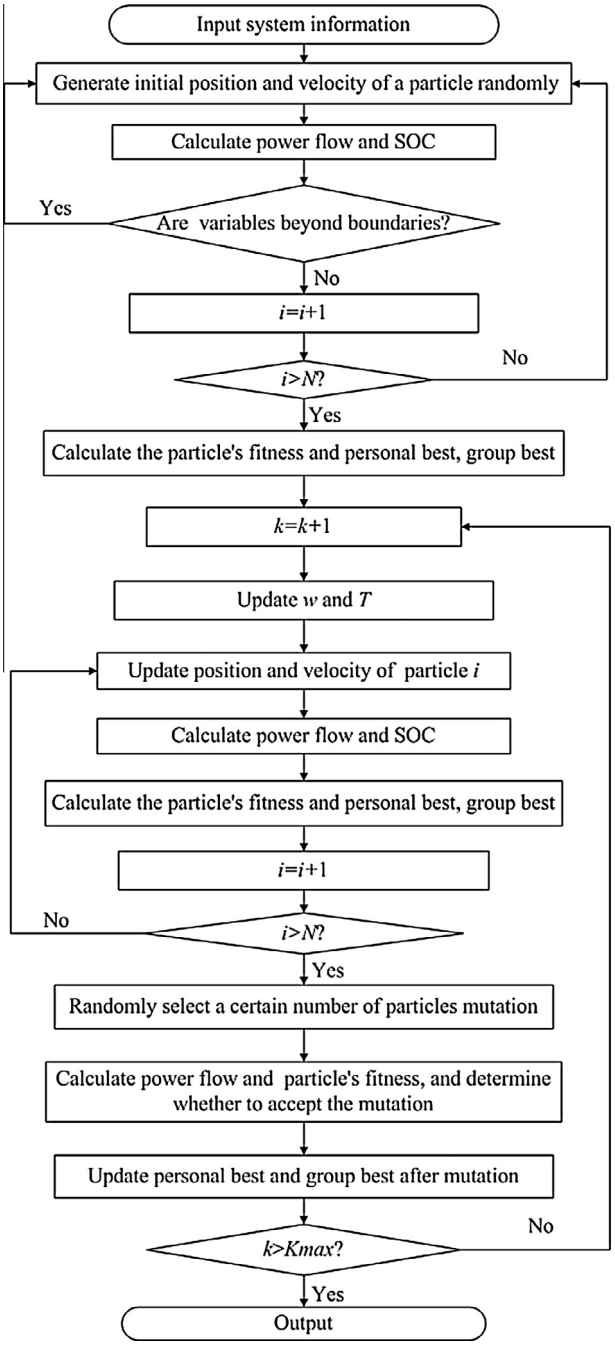

Fig. 2. The flowchart of the proposed strategy based on IPSO.

The flowchart of solving EVs charging and discharging strategy with IPSO is shown in Fig. 2.

4. Simulation analysis and results

4.1. Simulation system

To verify the effectiveness and feasibility of the charge–discharge strategy, a simulation of the practical distribution power grid in Kaili City in China is carried out, which is shown in Fig. 3. Node 10 is a slack bus, and there is an OLTC between node 10 and node 2. It is assumed that EVs obey the uniform distribution in the space and there are 10 EVs on each node. The simulation

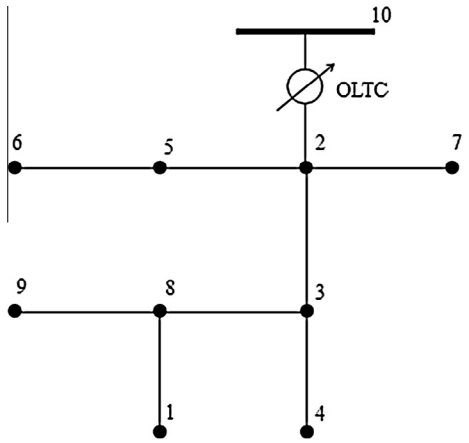

Fig. 3. The power grid model.

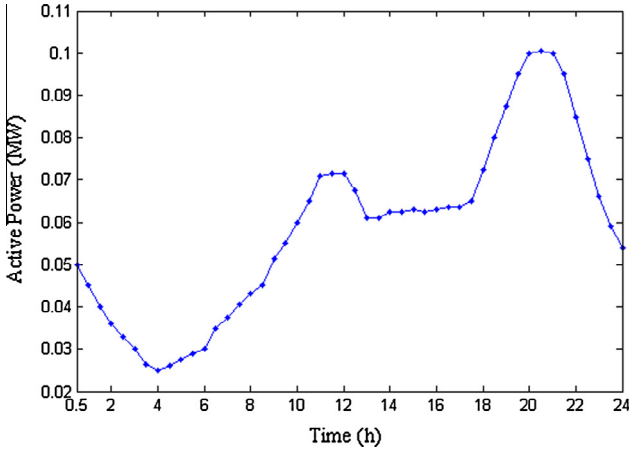

Fig. 4. A typical daily load curve.

adopts a per-unit system for calculation, in which the base capacity is 1 MVA, and the base voltage is 10 kV.

The simulation network is a 10 kV distribution power grid, in which the voltage of the slack bus is 10.5 kV (5% higher than the rated voltage). The allowable voltage range of node voltage is ±7% and the range of ratio adjustment of an OLTC is ±2 × 2.5%.

The total load of power grid can be divided into the basic load of its users and the charging load of the EVs. The basic load is known from the typical daily load curve shown in Fig. 4. To simplify the calculation, the 24-h day is divided into 48 intervals with each variable remaining constant in each time interval.

4.2. Unregulated charge simulation

When power grid operators do not control the charging behavior of EVs and EV owners' desire to charge their EVs, this charging mode can be called unregulated charging. In such uncoordinated charging scenario, initial charging time and charging period are affected by personal preference and other random factors. The only objective of charging is to get enough energy to satisfy the traveling need, and the effect of charging on power grid is ignored by EV owner. According to the theory of probability limit, the initial charging time of EVs can be considered to obey normal distribution. As people usually plug EV to the grid for charging when they reach home from work, the initial charging time follows the normal distribution $N(19, 1)$ [22,57]. It can be expressed as follows:

$$\varphi(t) = \frac{1}{\sqrt{2\pi}} e^{-\frac{(x-19)^2}{2}} \tag{25}$$

The total number of EVs in each node is N_{EV}, then the number of EVs connected to the grid to start charging is N_t in time interval $[t, t + \Delta t]$, and it can be expressed as follows.

$$N_t = N_{EV} \int_t^{t+\Delta t} \varphi(t)dt \tag{26}$$

The charging period will last generally 5–8 h [58], and it assumes that charging time for all EVs connected to the grid follows the uniform distribution in the interval [5,8]. The power grid is shown in Fig. 3, and the load is shown in Fig. 4. There are 10 EVs in each node. The parameters of the EVs [39] are based on the Nissan Leaf EV. The EV's charging power is constant and its value is 3.12 kW, and the capacity of the battery is 24 kW h.

A Monte Carlo simulation of the charging process for EVs is performed. As shown in Fig. 5, total charging load grows fast at 7:00 pm when is the peak period of electricity consumption in uncoordinated charging scenario, so the dumb charge will enlarge the peak-valley difference during 7:00–9:00 pm.

4.3. Optimal charging and discharging simulation

Comparing with the uncoordinated charging scenario, power grid operators can cooperate with EV owners on optimal charging to satisfy the needs of both power grid and EV owners. To investigate the benefit of the optimal charging strategy, simulations with the same power grid, the same load, the same EVs, the same numbers of EVs in each node, the same initial value of SOC and the same needs of traveling in a day are carried out.

According to literature [39], the EV's maximum charge and discharge power are both 3.12 kW and we assume that EVs charge and discharge continuously with maximal power. It is assumed that the time when EVs are disconnected from the power grid in the morning and afternoon obeys the normal distributions $N(7.5, 0.25)$ and $N(17.5, 0.25)$, respectively, and that the probability of EVs to disconnect from the power grid is 0.02 between the time 09:00 and 16:30. Therefore, the proportion of EVs connected to power grid at each moment in one day is calculated, as shown in Fig. 6.

The EVs' charging strategy is calculated by both traditional particle swarm optimization algorithm and IPSO algorithm, respectively. The parameters of the IPSO are shown in Table 2.

Learning factor c_1 and c_2 are used to control the impact of their own experience and group experience on their current speed respectively. Generally, c_1 is equal to c_2 and their value is between 0 and 4. In this paper, the value of c_1 and c_2 is 1.49445 [53,59]. w is called inertia weight factor which is non-negative, and it controls

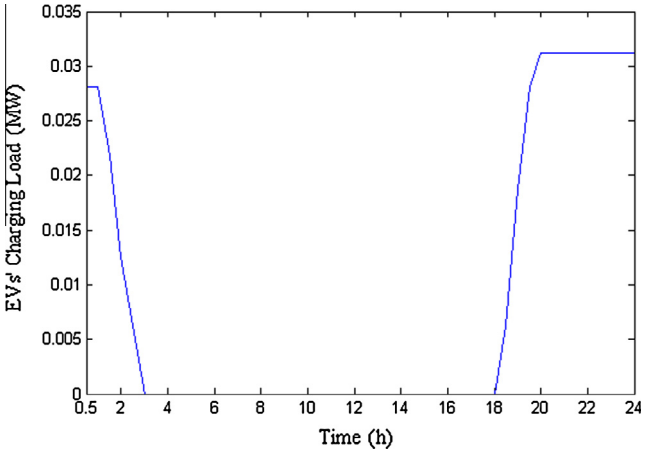

Fig. 5. Total charging load curve of EVs.

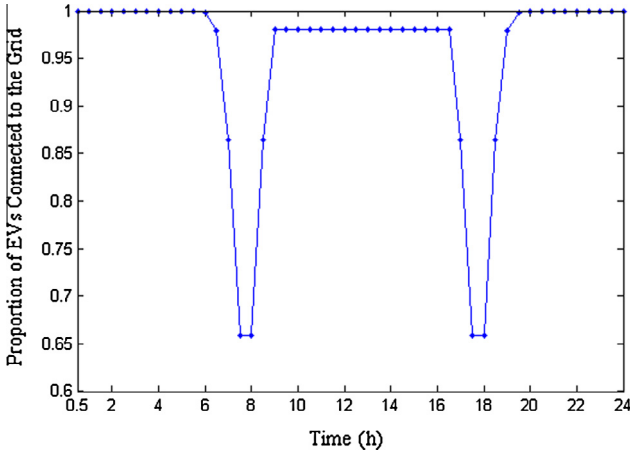

Fig. 6. The proportion of EVs connected to the power grid in one day.

Table 2
IPSO parameters.

Parameter	Symbol	Value
Learning factor	C_1	1.49445
Learning factor	C_2	1.49445
Maximum inertia factor	w_{max}	0.9
Minimum inertia factor	w_{min}	0.4
Population size	N	50
Mutation probability	P_m	0.2
Initial annealing temperature	T_0	1e6
Coefficient of cooling temperature	λ	0.9
Maximum number of iterations	k_{max}	1200

the impact of previous speed on the current speed. The previous speed has greater impact on the current speed and particles have better global search ability with larger w, while smaller w means less impact on the current speed and better local search ability of particles. w is descending between the range [60] of [0.4,0.9] according to linear decreasing rules in the search process. N is the population size of particles, and particles lack diversity with small N so that the algorithm will easily converge to local optimization. Also very large N will result in complex and meaningless calculation. In this paper, the value of N is defined as 50 [60]. P_m is the mutation probability and its value is defined as 0.2 to prevent local optimization and non-convergence in this paper. Simulated annealing algorithm accepts worse solution with a certain probability. The initial temperature should be sufficiently high so that the probability of receiving a worse solution is high. Then the temperature is gradually reduced to decrease the probability gradually, and it will improve the diversity of particles in the population in the beginning of calculation. If the initial temperature is not high enough or falling too fast, it is not conducive to global optimization. And temperature must be slowly cooled, so the cooling factor λ is close to 1. According to literature [55], T_0 = 1e6, and $\lambda = 0.9$. In one iteration of the PSO algorithm, the temperature declines with the rate of 90% and 20% of particles mutate in each iteration, then the acceptance of new mutation particles will be determined according to Eqs. (22) and (23). The algorithm does not converge with less iterations, while more iterations increase

Table 3
The objective function value of traditional PSO and IPSO.

	Best value	Worst value	Average value	Variance value
Traditional PSO	0.6115	0.8782	0.7195	0.0055
IPSO	0.5721	0.7765	0.6716	0.0023

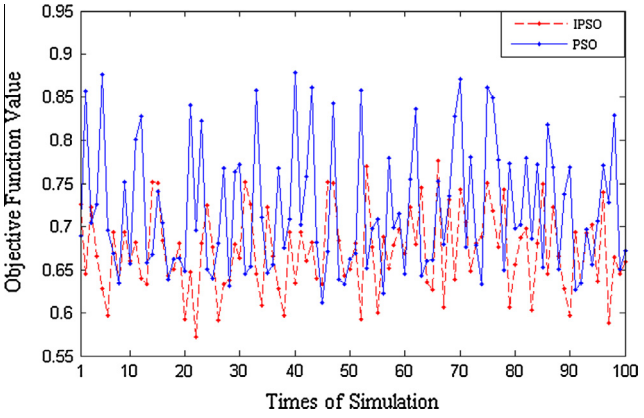

Fig. 7. The distribution of objective function value in simulation.

computation complexity, so the maximum iterations are 1200. The maximum flight speed of particles is $|u_{d,max} - u_{d,min}|$ [60].

Both the IPSO and traditional PSO are repeated for 100 times, and the results are showed in Table 3 and Fig. 7. In Fig. 7, IPSO has better performance on best optimization value, worst optimization value and average value. Also, the probability of optimized solution in IPSO is greater than that in traditional PSO. Because the optimization model for EVs charging and discharging includes a number of control variables, the algorithm requires a number of iterations (i.e., 1200) to converge. As shown in Fig. 8, the objective function value of IPSO is larger than PSO's with lower decreasing speed in the middle of the convergence process. The particles accept the worse solution with a large probability, so the diversity of particles will increase. According to Eq. (23), the probability of accepting worse solution becomes very small as iterations increase and annealing temperature decrease. So that IPSO can finally converge to a smaller objective function than PSO with fast convergence rate. Table 3 shows that the IPSO can achieve about 6% decrease in objective function value, which means obvious economic benefit. For example, Kaili city consumes electricity of about 6 billion kW h per year, and the percentage of its network losses is about 4.0%. The electricity price is 0.538 CNY per kW h, so 6% decrease of objective function value means that the network loss will reduce at least two million CNY per year.

To investigate the statistical significance of the global optimal ability of the proposed IPSO, two-sample t-tests are carried out based on the simulation results. We assume that $X_1, X_2, \ldots, X_{100}$ and $Y_1, Y_2, \ldots, Y_{100}$ are objective function values obtained by

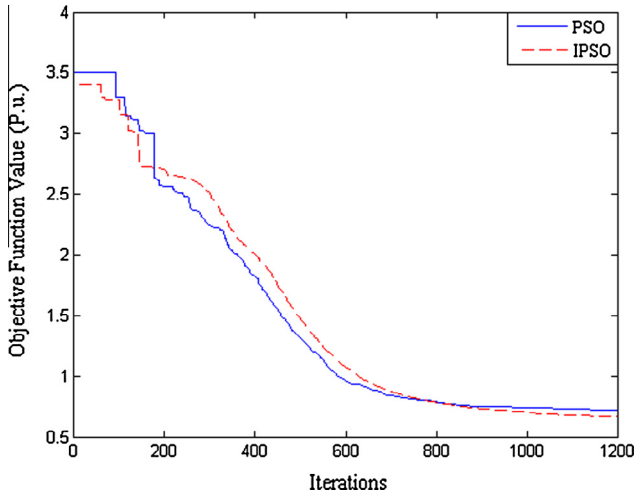

Fig. 8. The convergence curve of traditional PSO and IPSO.

running IPSO and traditional PSO for 100 times respectively. They are samples from normal population $X \sim N(\mu_1, \sigma_1^2)$ and $Y \sim N(\mu_2, \sigma_2^2)$, $\bar{x}$ and $\bar{y}$ are the mean of $X_1, X_2, \ldots, X_{100}$ and $Y_1, Y_2, \ldots, Y_{100}$ respectively. Statistical hypothesis are $H_0 : \mu_1 \geqslant \mu_2$ and $H_1 : \mu_1 < \mu_2$. The significant level is set as 0.05 [61], thus the rejection region is $\{\bar{x} - \bar{y} < -0.0148\}$ according to t-distribution. Because $\bar{x} - \bar{y} = -0.0479 < -0.0148$, H_0 should be rejected and H_1 should be accepted. So the average value of IPSO is less than that of traditional PSO from the view of statistics, which means the IPSO has better ability than traditional PSO to find global optimal solution.

Based on the 100 independent simulation results, we calculate the average value of the objective function, SOC, ratio of OLTC, active load and network losses, among others.

The SOC curve of the EV at node 8 is shown in Fig. 9. Because this paper does not involve charging tariff, end-user cost does not be considered. As shown in Fig. 9, SOC is closer to 1 at 7:00 am considering owner's DoS than without it. EV owner's DoS increases because the SOC in proposed strategy is much higher than that without considering DoS, then longer traveling distance can be obtained. The final value of SOC in a day is the initial value of next day. In the next day, EVs charging and discharging plan will be recalculated according to that day's initial SOC and other information. So the initial and final SOC values do not need to be the same. Also the arrangement of next day needs to be re-simulated according to the input of the next day.

To simplify the calculation, the ratio of an OLTC changes continuously in the range from 0.95 to 1.05 in the simulation, while the adjustment range of the actual ratio should be $\pm 2 \times 2.5\%$. In practice, the OLTC tap is only fixed at the closest ratio to the five discrete values, including 0.95, 0.975, 1, 1.025 and 1.05.

The optimized ratio of an OLTC is shown in Fig. 10, in which no adjustment of the OLTC is needed after the optimization at a peak load.

The daily load curve of the slack bus 10 is shown in Fig. 11, which also represents the daily load curve of the entire distribution network. Without any EVs charging, the peak load is 1.2011 MW, the valley (minimum) load is 0.2925 MW, and the peak-to-valley difference is 0.9086 MW, whereas they are changed to 1.0280 MW, 0.4786 MW and 0.5494 MW, respectively, with the optimal charging and discharging of EVs. As shown, the optimized strategy of the charging and discharging of EVs has a better performance on the power valleys and peaks than no EVs and uncoordinated charging.

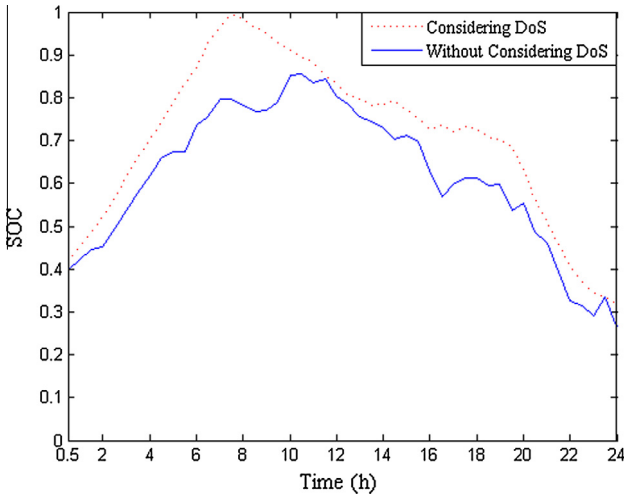

Fig. 9. An electric vehicle's SOC.

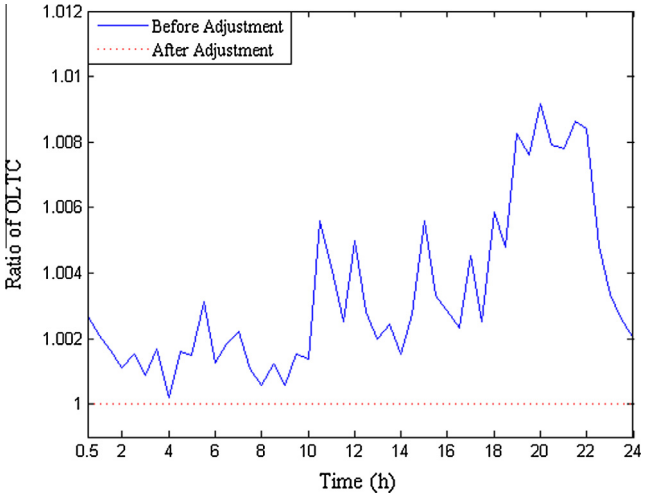

Fig. 10. The transformation ratio of OLTC.

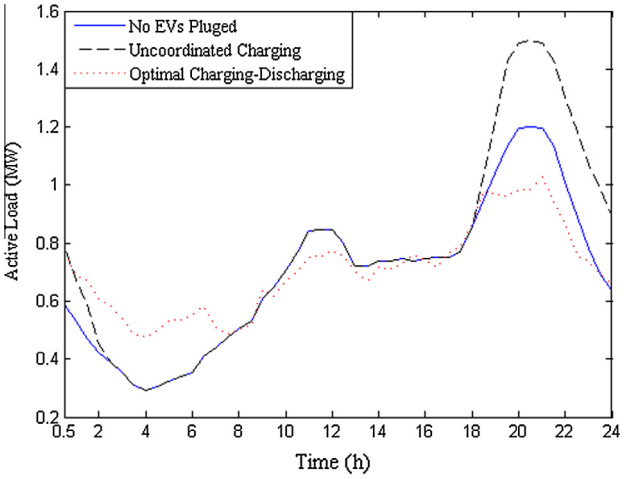

Fig. 11. The daily load curve of the whole power grid.

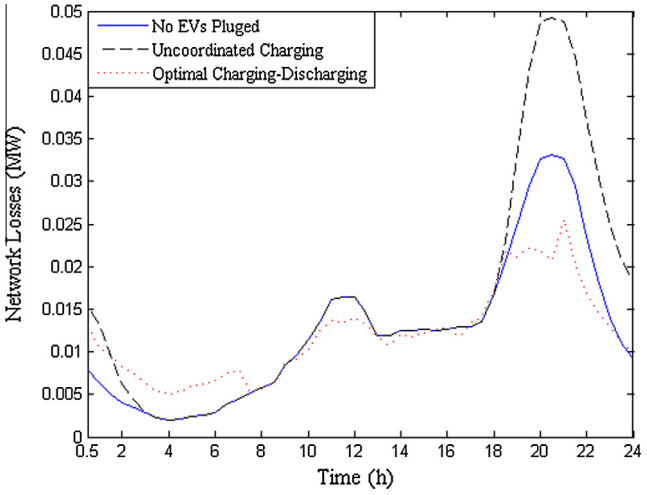

Fig. 12. The active power loss of power grid.

The transmission loss curves of the network before and after EVs are connected to the grid are shown in Fig. 12. The total transmission loss of one day is 0.5975 MW without any EVs connected

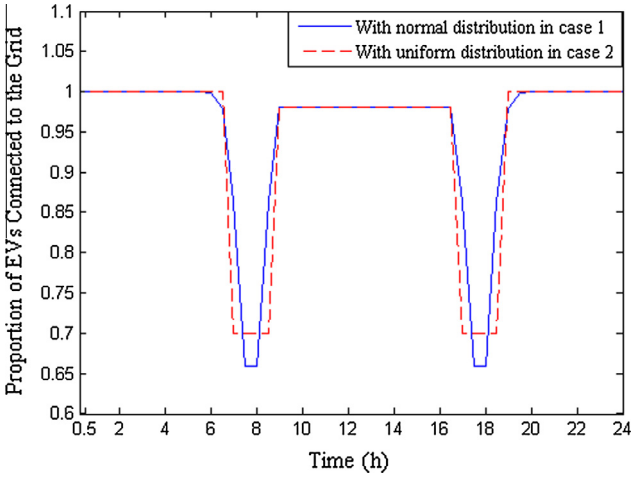

Fig. 13. The proportion of EVs connected to the grid.

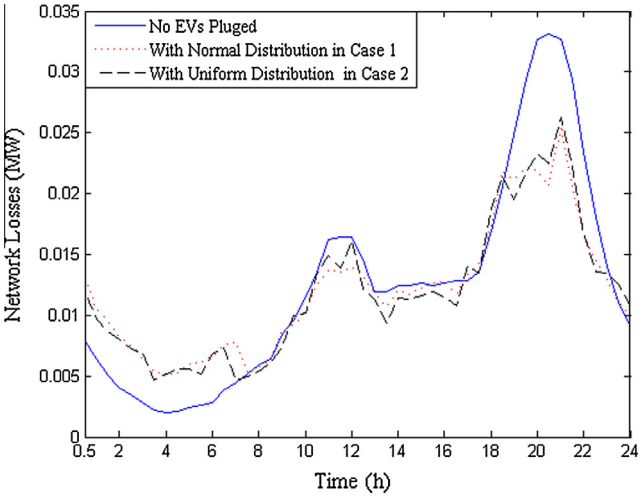

Fig. 15. The active power loss of power grid.

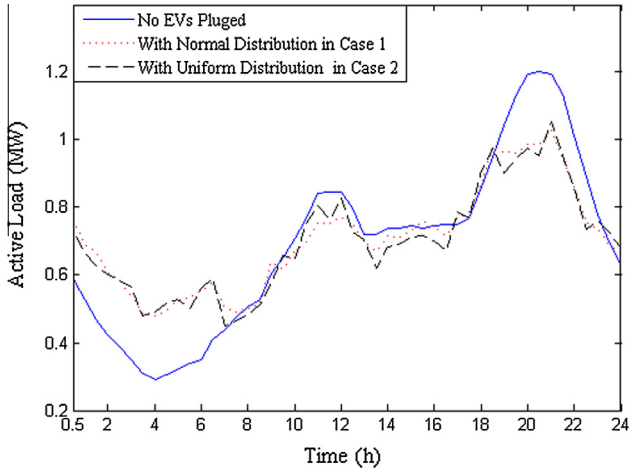

Fig. 14. The daily load curve of the whole power grid.

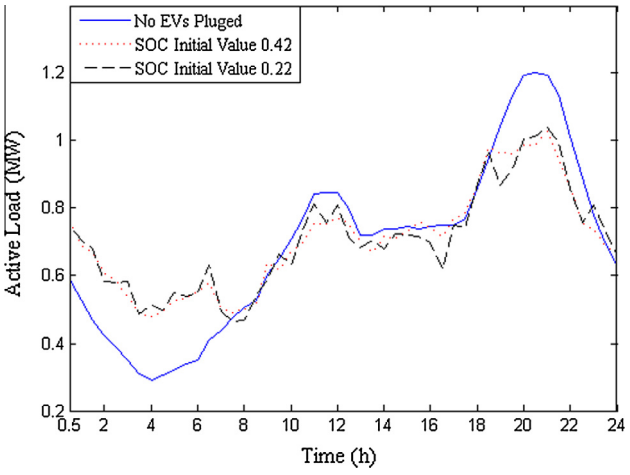

Fig. 16. The daily load curve of the whole power grid.

to the power grid, which will be 0.7627 MW when EVs are charging in an uncoordinated manner. The total transmission loss changes to 0.5771 MW after the power grid operator controls EVs to charge and discharge by the optimal charging strategy. As a result, the transmission loss is reduced to 24.3% less than the loss of uncoordinated charging.

4.4. The impact of probability distribution

To investigate the impact of probability distribution on optimization, simulations of different distributions are carried out. The proportion of EVs connected to power grid at each moment in one day is presented in Fig. 13. The time when EVs are disconnected from the power grid in the morning and afternoon obeys the normal distributions $N(7.5, 0.25)$ and $N(17.5, 0.25)$ respectively in case 1, also the probability of EVs disconnecting from the power grid during 09:00–16:30 is 0.02. The time when EVs are disconnected from the power grid in the morning and afternoon obeys the uniform distribution in case 2, and the probability is 0.3. The probability of EVs disconnecting from the power grid during 09:00–16:30 in case 2 is 0.02 too. Figs. 14 and 15 show that the optimal results of active load and network loss have little difference between normal distribution and uniform distribution. So EVs have almost no impact on the optimization results no matter what kind of distributions is used.

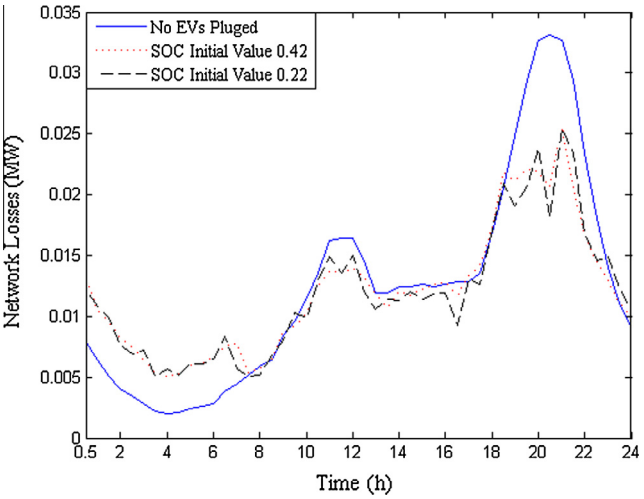

Fig. 17. The active power loss of power grid.

4.5. The impact of the initial value of SOC

The initial value of SOC is given randomly in this paper. To investigate whether the initial value of SOC has an obvious impact

on the result, simulation is repeated with different initial values of SOC. As shown in Figs. 16 and 17, the initial value of SOC has little impact on the optimal results.

5. Conclusions

The large development of electric vehicles brings us to the concern of the impacts on the electricity grid. However, if large numbers of EVs connect to the grid simultaneously, there could be a wide variety of impacts to the grid. Based on the random manner in which EVs are connected to the power grid, EV charging models are analyzed with the accessing time character. Simulation results show that uncoordinated charging of EVs enlarges peak-to-valley difference and active power loss of power grid, which is caused by charging load of EVs.

So the arrangement of the charging or discharging of EVs connected to a power grid must be regulated with the increasing commercial application of EVs. Considering the constraints of power grid operation and battery function, an optimal power flow based EV charging and discharging strategy is proposed to improve the economic and technical performance of power grid operation. It is clear that optimal scheduling of charging provides significant benefits to all involved. Comparing with the uncoordinated charging and non-EV-accession, results from this work have shown that the peak-to-valley difference and active power loss are obviously reduced, together with increased DoS of EV owners and reduced adjustment frequencies of the OLTC. Also, different distributions of EVs connecting time and different initial-values of SOC have no impact on the optimized results.

An improved particle swarm optimization (IPSO) algorithm based on genetic variation and simulated annealing is developed to solve the optimization of charging and discharging of EVs. And, better performance on the global search capability and optimal result of the IPSO algorithm is verified.

Future work will involve low carbon, renewable generations and layer-by-layer optimization for a large number of EVs in the power grid.

Acknowledgments

The work is funded by the National Science Foundation of China (51277135, 50707021) and Special Funds for Projects of Basic Research and Operational Costs of the Central Universities.

References

[1] Foley Aoife, Tyther Barry, Calnan Patrick, Gallachóir Brian Ó. Impacts of electric vehicle charging under electricity market operations. Appl Energy 2013;101(January):93–102.
[2] Saxena Samveg, Gopal Anand, Phadke Amol. Electrical consumption of two-, three- and four-wheel light-duty electric vehicles in India. Appl Energy 2014;115:582–90.
[3] Khayyam Hamid, Abawajy Jemal, Javadi Bahman, Goscinski Andrzej, Stojcevski Alex, Bab-Hadiashar Alireza. Intelligent battery energy management and control for vehicle-to-grid via cloud computing network. Appl Energy 2013;111:971–81.
[4] Saarenpää Jukka, Kolehmainen Mikko, Niska Harri. Geodemographic analysis and estimation of early plug-in hybrid electric vehicle adoption. Appl Energy 2013;107:456–64.
[5] Sorrentino Marco, Rizzo Gianfranco, Sorrentino Luca. A study aimed at assessing the potential impact of vehicle electrification on grid infrastructure and road-traffic green house emissions. Appl Energy 2014;120:31–40.
[6] Han Sekyung, Han Soohee, Aki Hirohisa. A practical battery wear model for electric vehicle charging applications. Appl Energy 2014;113:1100–8.
[7] Millo Federico, Rolando Luciano, Fuso Rocco, Mallamo Fabio. Real CO_2 emissions benefits and end user's operating costs of a plug-in Hybrid Electric Vehicle. Appl Energy 2014;114:563–71.
[8] Bartolozzi I, Rizzi F, Frey M. Comparison between hydrogen and electric vehicles by life cycle assessment: a case study in Tuscany, Italy. Appl Energy 2013;101:103–11.
[9] Shu Zhang, Zechun Hu, Yonghua Song. Research on unit commitment considering interaction between battery swapping station and power grid. Proc CSEE 2012;32(10):49–55.
[10] Fernandes Camila, Frías Pablo, Latorre Jesús M. Impact of vehicle-to-grid on power system operation costs: the Spanish case study. Appl Energy 2012;96:194–202.
[11] Sousa Tiago, Morais Hugo, Soares João, Vale Zita. Day-ahead resource scheduling in smart g rids considering vehicle-to-grid and network constraints. Appl Energy 2012;96(August):183–93.
[12] Dallinger David, Gerda Schubert, Wietschel Martin. Integration of intermittent renewable power supply using grid-connected vehicles – a 2030 case study for California and Germany. Appl Energy 2013;104:666–82.
[13] Brouwer Anne Sjoerd, Kuramochi Takeshi, Broek Machteld van den, Faaij André. Fulfilling the electricity demand of electric vehicles in the long term future: an evaluation of centralized and decentralized power supply systems. Appl Energy 2013;107:33–51.
[14] Su Wencong, Chow Mo-Yuen. Computational intelligence-based energy management for a large-scale PHEV/PEV enabled municipal parking deck. Appl Energy 2012;96:171–82.
[15] Trovao JP, Pereirinha PG, Trovao L, et al. Electric vehicles chargers characterization: load demand and harmonic distortion. In: 11th International conference on electrical power quality and utilisation (EPQU), 2011. Lisbon; 2011. p. 1–7.
[16] Monteiro V, Goncalves H, Afonso JL. Impact of electric vehicles on power quality in a smart grid context. In: 11th International conference on electrical power quality and utilisation (EPQU), 2011. Lisbon; 2011. p. 1–6.
[17] Akhavan-Rezai E, Shaaban MF, El-Saadany EF, et al. Uncoordinated charging impacts of electric vehicles on electric distribution grids: normal and fast charging comparison. In: IEEE power and energy society general meeting, 2012. San Diego, CA; 2012. p. 1–7.
[18] Dharmakeerthi CH, Mithulananthan N, Saha TK. Overview of the impacts of plug-in electric vehicles on the power grid. In: IEEE PES innovative smart grid technologies Asia (ISGT), 2011. Perth, WA; 2011. p. 1–8.
[19] Weis Allison, Jaramillo Paulina, Michalek Jeremy. Estimating the potential of controlled plug-in hybrid electric vehicle charging to reduce operational and capacity expansion costs for electric power systems with high wind penetration. Appl Energy 2014;115:190–204.
[20] Trovao L, Jorge HM. Power demand impacts of the charging of electric vehicles on the power distribution network in a residential area. Proceedings of the 2011 3rd International Youth Conference on Energetics (IYCE). Leiria; 2011. p. 1–6.
[21] Liting Tian, Shuanglong Shi, Zhuo Jia. A statistical model for charging power demand of electric vehicles. Power System Technol 2010;34(11):126–30.
[22] Ciwei Gao, Liang Zhang. Overview of the impact of electric vehicle charging on power grid. Power System Technol 2011;35(2):127–31.
[23] Trovão João P, Pereirinha Paulo G, Jorge Humberto M, Antunes Carlos Henggeler. A multi-level energy management system for multi-source electric vehicles – an integrated rule-based meta-heuristic approach. Appl Energy 2013;105(May):304–18.
[24] Ruqi Li, Haoyi Su. Optimal allocation of charging facilities for electric vehicle based on queuing theory. Automation Electric Power Syst 2011;35(14):58–61.
[25] Zhiwei Xu, Zechun Hu, Yonghua Song. Coordinated charging of plug-in electric vehicles in charging stations. Automation Electric Power Syst 2012;36(11):38–43.
[26] Ruisheng Li, Xiaolei Wang, Fengquan Zhou. The system of electric vehicle intelligence charge station with smart power flow control. Power System Protect Control 2010;38(21):87–90.
[27] Junhua Zhao, Fushuan Wen, Yusheng Xue. Power system stochastic economic dispatch considering uncertain outputs from plug-in electric vehicles and wind generators. Automation Electric Power Syst 2010;34(20):22–9.
[28] Wen Zou, Fubao Wu, Zhihong Liu. Centralized charging strategies of plug-in hybrid electric vehicles under electricity markets based on spot pricing. Automation Electric Power Syst 2011;35(14):62–7.
[29] Zhengshuo Li, Hongbin Su, Qinglai Guo. Study on wind-EV complementation on the transmission Grid side considering carbon emission. Proc CSEE 2012;32(10):7–41.
[30] Meiqin Mao, Shujuan Sun, Jianhui Su. Economic analysis of a microgrid with wind/photovoltaic/storages and electric vehicles. Automation Electric Power Syst 2011;35(14):30–5.
[31] Qiuna Cai, Fushuan Wen, Yusheng Xue. An SCUC-based optimization approach for power system dispatching with plug-in hybrid electric vehicles. Automation Electric Power Syst 2012;36(1):38–46.
[32] Weifeng Yao, Junhua Zhao, Fushuan Wen. A charging and discharging dispatching strategy for electric vehicles based on bi-level optimization. Automation Electric Power Syst 2012;36(11):30–7.
[33] Kaiqiao Zhan, Yonghua Song, Zechun Hu. Coordination of electric vehicle charging to minimize active power losses. Proc CSEE 2012;32(31):11–8.
[34] Zhuowei Luo, Zhuowei Hu, Yonghua Song. Study on charging load modeling and coordinated charging of electric vehicles under battery swapping modes. Proc CSEE 2012;32(31):1–10.
[35] Mets Kevin, Verschueren Tom, Haerick Wouter. Optimizing smart energy control strategies for plug-in hybrid electric vehicle charging. In: 2010 IEEE/IFIP network operations and management symposium workshops, NOMS 2010. Osaka, Japan; 2010. p. 293–99.
[36] Ferreira Joao C, Afonso Joao Luiz. Towards a collective knowledge for a smart electric vehicle charging strategy. IEEE 3rd international conference on communication software and networks (ICCSN), 2011; 2011. p. 735–39.

[37] Niklas Rotering, Marija Ilic. Optimal charge control of plug-in hybrid electric vehicles in deregulated electricity markets. IEEE Trans Power Syst 2011;26(3):1021–9.
[38] Acha Salvador, Green Tim C, Shah Nilay. Effects of optimised plug-in hybrid vehicle charging strategies on electric distribution network losses. In: 2010 IEEE PES transmission and distribution conference and exposition: smart solutions for a changing world. New Orleans, LA, United states; 2010. p. 1–6.
[39] Acha S, Green TC, Shah N. Optimal charging strategies of electric vehicles in the UK power market. Innovative Smart Grid Technologies (ISGT), 2011 IEEE PES; 2011. p. 1–8.
[40] Acha Salvador, Green Tim C, Shah Nilay. Impacts of plug-in hybrid vehicles and combined heat and power technologies on electric and gas distribution network losses. In: 1st IEEE-PES/IAS conference on sustainable alternative energy, SAE 2009 – Proceedings. Valencia, Spain, 2009, pp. 1–7.
[41] He Yifeng, Venkatesh Bala, Guan Ling. Optimal scheduling for charging and discharging of electric vehicles. IEEE Trans Smart Grid 2012;3(3):1095–2015.
[42] Richardson Peter, Flynn Damian, Keane Andrew. Optimal charging of electric vehicles in low-voltage distribution systems. IEEE Trans Power Syst 2012;27(1):268–79.
[43] Jin Chenrui, Tang Jian, Ghosh P. Optimizing electric vehicle charging with energy storage in the electricity market. IEEE Trans Smart Grid 2013;4(1):311–20.
[44] Kristoffersen Trine Krogh, Capion Karsten, Meibom Peter. Optimal charging of electric drive vehicles in a market environment. Appl Energy 2011;88(5):1940–8.
[45] Sortomme Eric, El-Sharkawi Mohamed A. Optimal scheduling of vehicle-to-grid energy and ancillary services. IEEE Trans Smart Grid 2012;3(1):351–9.
[46] Cao Yijia, Tang Shengwei, et al. An optimized EV charging model considering TOU price and SOC curve. IEEE Trans Smart Grid 2012;3(1):388–93.
[47] Sundström Olle, Binding Carl. Flexible charging optimization for electric vehicles considering distribution grid constraints. IEEE Trans Smart Grid 2012;3(1):26–37.
[48] Han Sekyung, Han Soohee, Sezaki K. Development of an optimal vehicle-to-grid aggregator for frequency regulation. IEEE Trans Smart Grid 2010;1(1):65–72.
[49] Bashash Saeid, Moura Scott J, Forman Joel C, Fathy Hosam K. Plug-in hybrid electric vehicle charge pattern optimization for energy cost and battery longevity. J Power Sources 2011;196(1):541–9.
[50] Plett Gregory L. Extended Kalman filtering for battery management systems of LiPB-based HEV battery packs: Part 3. State and parameter estimation. J Power Sources 2004;134(2):277–92.
[51] Yuryevich J, Wong KP. Evolutionary programming based optimal power flow algorithm. IEEE Trans Power Syst 1999;14(4):1245–50.
[52] Bakirtzis AG, Biskas PN, Zoumas CE, et al. Optimal power flow by enhanced genetic algorithm. IEEE Trans Power Syst 2002;17(2):229–36.
[53] Bo Yang, Zunlian Zhao, Yunping Chen. An improved particle swarm optimization algorithm for optimal power flow problem. Power System Technol 2006;30(11):6–10.
[54] Guimin Chen, Jianyuan Jia, Qi Han. Study on the strategy of decreasing inertia weight in particle swarm optimization algorithm. J Xi'an Jiaotong Univ 2006;40(1):53–6. 61.
[55] Ying Gao, Shengli Xie. Particle swarm optimization algorithms based on simulated annealing. Comput Eng Appl 2004;40(1):47–50.
[56] Jianchao Zeng, Zhihua Cui. A guaranteed global convergence particle swarm optimizer. J Comput Res Develop 2004;41(8):1333–8.
[57] Li Lei, Quanbin Liu. Discussion on the impact of electric vehicle on the grid load curve. Electrical Mach Technol 2000;1:37–9.
[58] Koyanagi F, Uriu Y. Modeling power consumption by electric vehicles and its impact on power demand. Electrical Eng Japan 1997;120(4):40–7.
[59] Maurlce Clerc. The swarm and the queen: towards a deterministic and adaptive particle swarm optimization. Proc IEEE Congr Evolut Comput 1999:1951–7.
[60] Zanmei Yu. Application of improved particle swarm optimization for optimal power flow. Baoding: North China Electric Power University; 2006.
[61] Chen WN, Zhang J, Lin Y, et al. Particle swarm optimization with an aging leader and challengers. IEEE Trans Evolut Comput 2013;17(2):241–58.